Supporting information

Boosting the bifunctional electrocatalytic performance of nanowire $NiCo_2O_4$@ultrathin porous carbon via modulating d-band center

Huiqin Yu [a], Fang Li [a*], Jing Cao [a], Shifu Chen [a], Haili Lin [a*]

[a] Key Laboratory of Green and Precise Synthetic Chemistry and Applications, Ministry of Education; College of Chemistry and Materials Science, Huaibei Normal University, Huaibei, Anhui 235000, P. R. China

*Corresponding author.

E-mail address: lifang14@mails.ucas.ac.cn (Fang Li); linhaili@mail.ipc.ac.cn (Haili Lin)

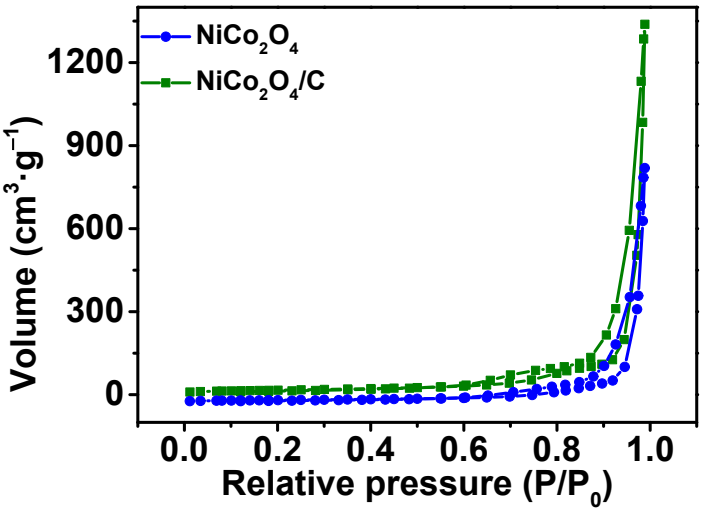

Figure S1. N_2 adsorption-desorption isotherms of $NiCo_2O_4$ and $NiCo_2O_4$/C.

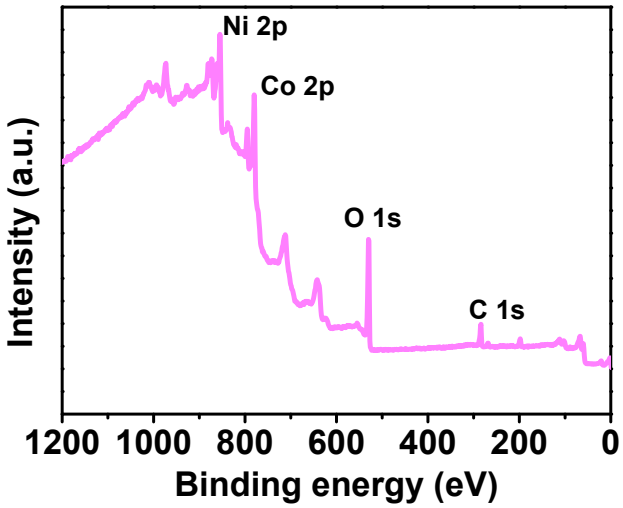

Figure S2. XPS full survey spectrum of $NiCo_2O_4$/C sample.

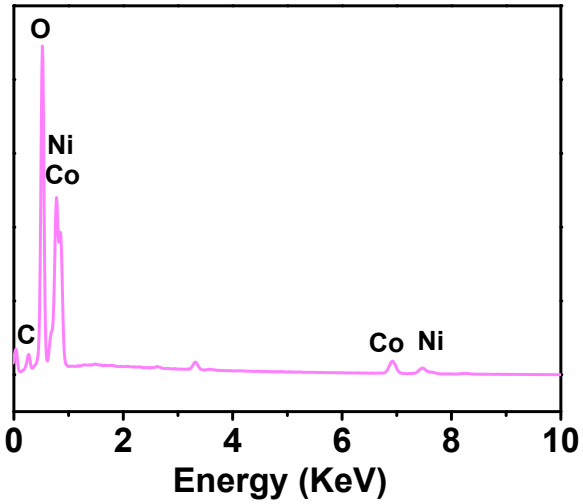

Figure S3. Energy Dispersive Spectrometer of the $NiCo_2O_4$/C.

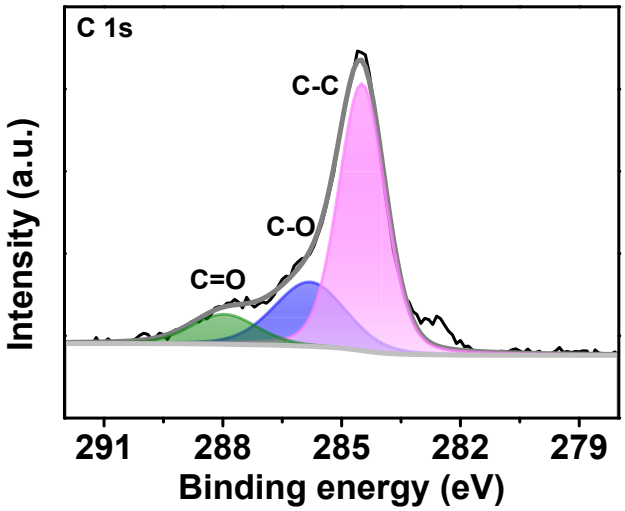

Figure S4. High-resolution C 1s XPS spectra of the $NiCo_2O_4$/C/NF.

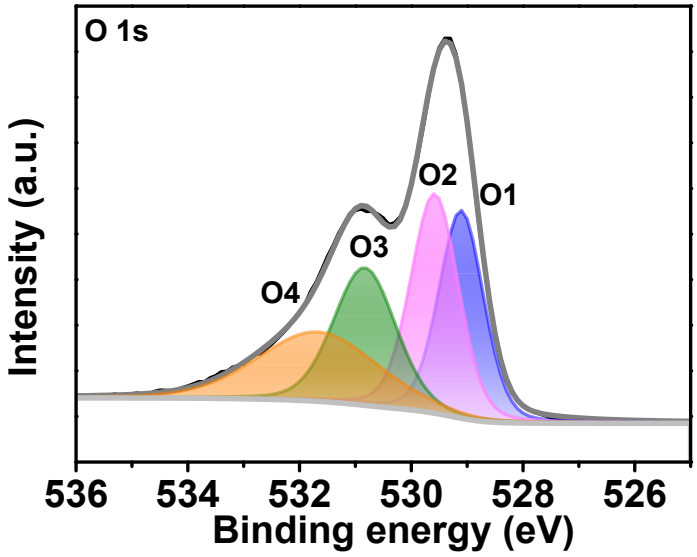

Figure S5. High-resolution O 1s XPS spectra of the $NiCo_2O_4$/C/NF.

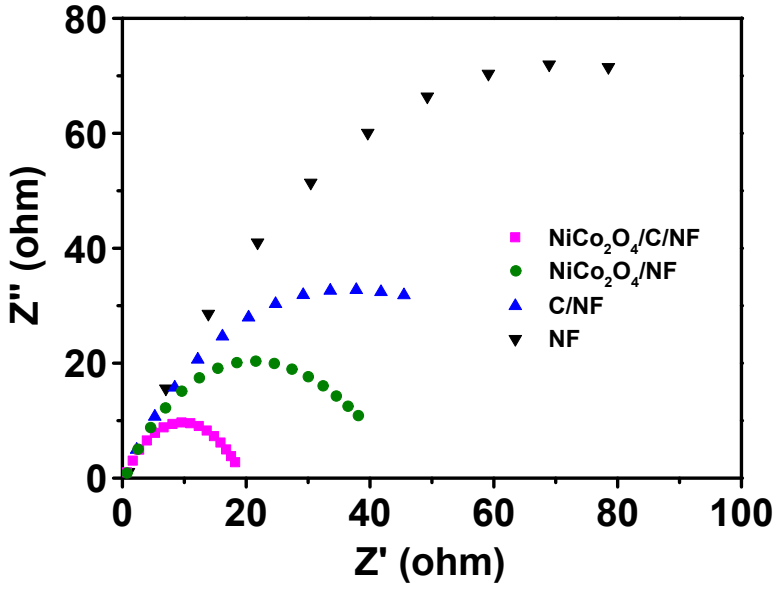

Figure S6. The EIS of the $NiCo_2O_4$/C/NF, $NiCo_2O_4$/NF, C/NF, and NF.

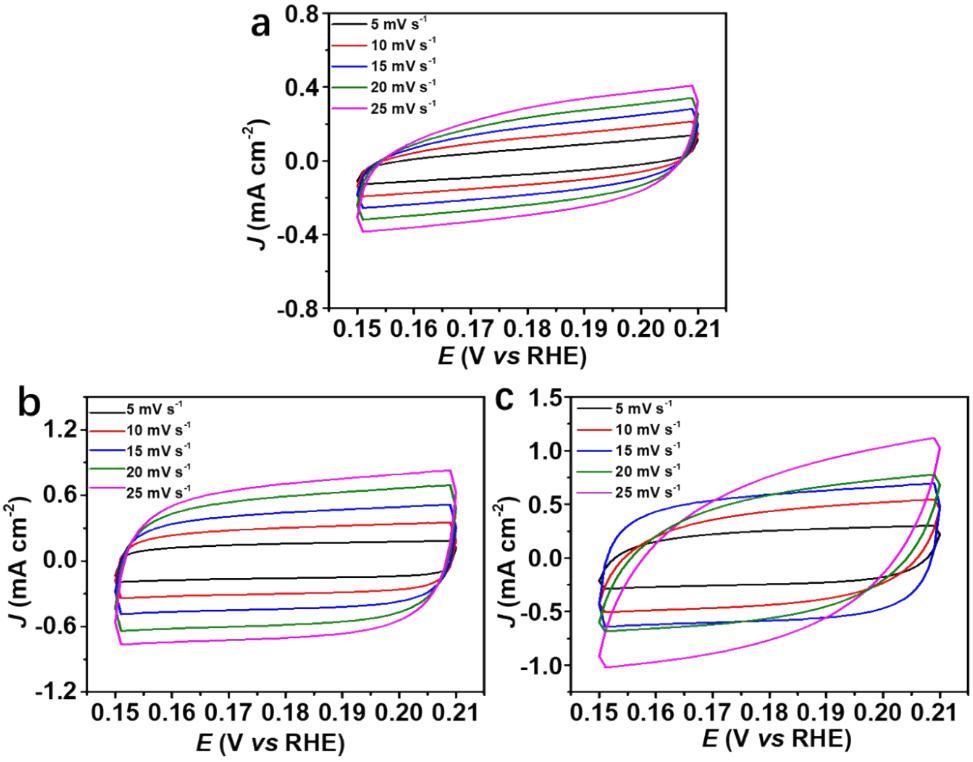

Figure S7. The CV of the $NiCo_2O_4$/C/NF, $NiCo_2O_4$/NF, and C/NF.

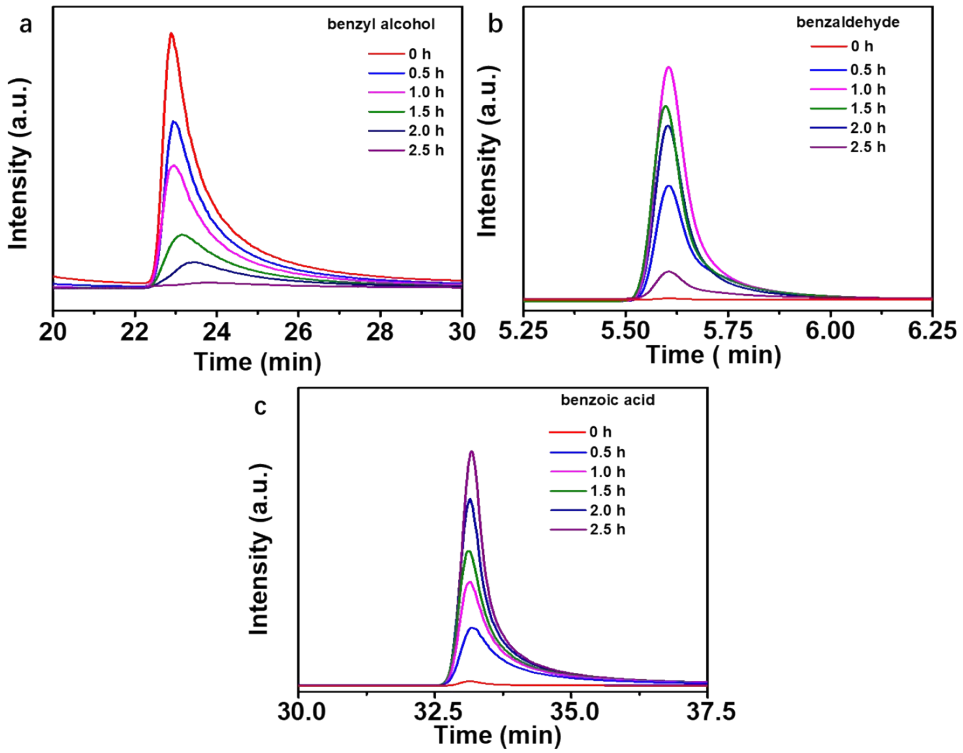

Figure S8. The HPLC result of the $NiCo_2O_4$/C/NF, $NiCo_2O_4$/NF, and C/NF.

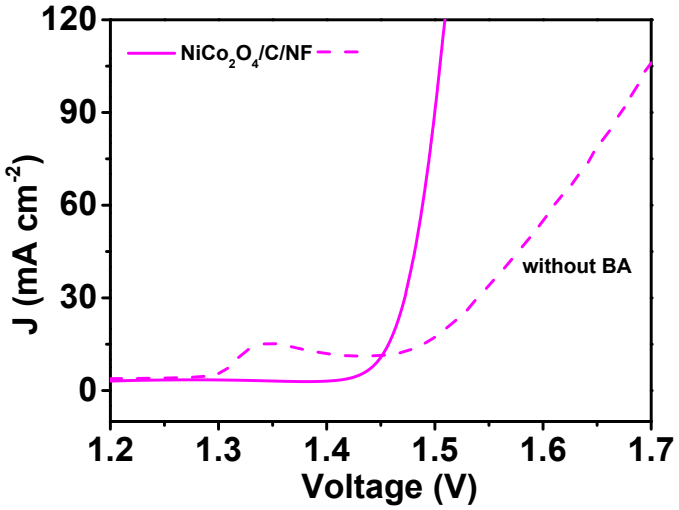

Figure S9 The comparison of whole reaction in BA electrolyte and overall water-splitting reaction in electrolyte free of BA.

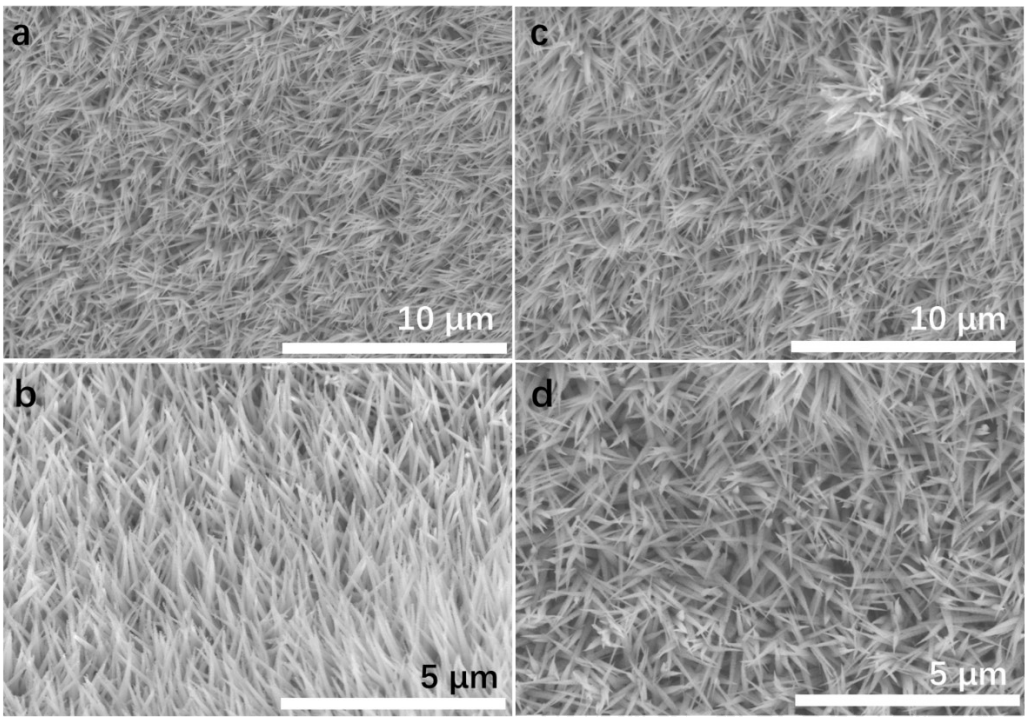

Figure S10. The SEM after long-term HER (a and b) and BA oxidation (c and d).

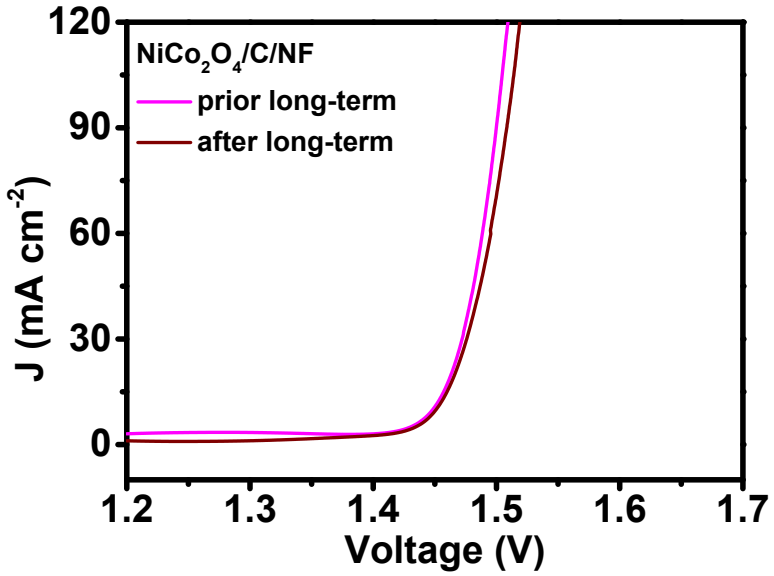

Figure S11 The LSV curve before and after long term whole reaction.

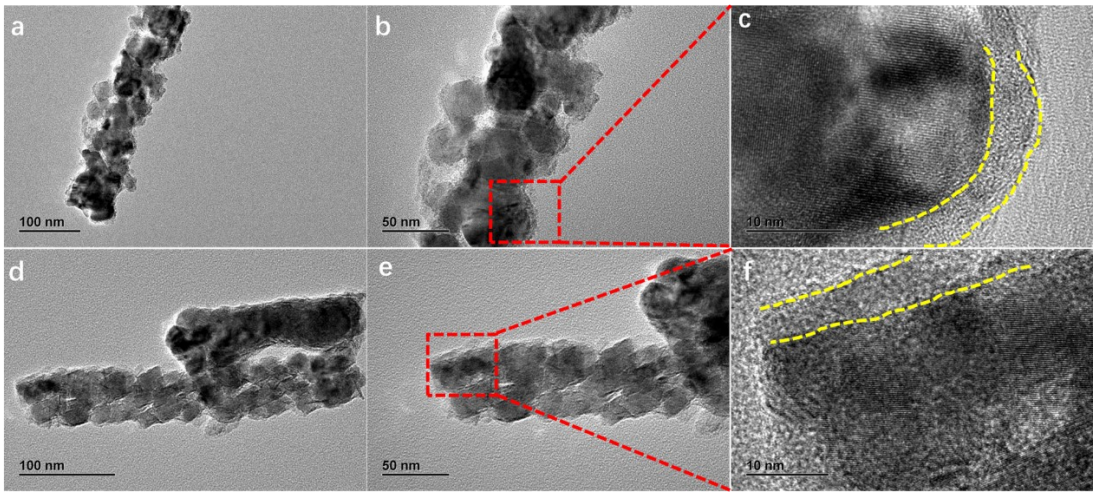

Figure S12 The TEM for the long-term HER (a, b, and c) and BA oxidation (d, e, and f)

Table S1 Comparison of HER property

Catalyst	Electrolyte	Overpotential (10 mA cm^{-2})	Ref.
Vc-FeP	1 M KOH	108	1
$CoSe_2$/a-CoP	1 M KOH	151	2
NiCo-LDH@$Cu(OH)_2$/CF	1 M KOH	263	3
Co-Co_2C/CC	1 M KOH	96	4
Co_2P	1 M KOH	190	5
NiFe alloy	1 M KOH	236	6
Co_2FeO_4@PdO	1 M KOH	269	7
Ni@NCS-800	1 M KOH	330	8
Cu–Ni (1:1) @NRG	1 M KOH	107	9
Fe-Ni_3S_2/Ni_2P	1 M KOH	112	10
C@NiCo12	1 M KOH	105	11
MoS_2	1 M KOH	248	12
Co-Mo_2C-0.020	1 M KOH	140	13
W_2N/WC	1 M KOH	148.5	14
CoP-NC@NFP	1 M KOH	162	15
Ni_5P_4/Ni_2P/Fe_2P-2	1 M KOH	190	16

[1] W.L. Kwong, E. Gracia-Espino, C.C. Lee, R. Sandström, T. Wågberg, J. Messinger, Cationic vacancy defects in iron phosphide: a promising route toward efficient and stable hydrogen evolution by electrochemical water splitting, ChenSusChem 10 (2017) 4544-4551.

[2] S.J. Shen, Z.P. Wang, Z.P. Lin, K. Song, Q.H. Zhang, F.Q. Meng, L. Gu, W.W. Zhong, Crystalline-amorphous interfaces coupling of $CoSe_2$/CoP with optimized d-band center and boosted electrocatalytic hydrogen evolution, Adv. Mater. 34 (2022) 2110631.

[3] P.Y. Wang, J.W. Zhu, Z.H. Pu, R. Qin, C.T. Zhang, D. Chen, Q. Liu, D.L. Wu, W.Q. Li, S.L. Liu, J.S. Xiao, S.C. Mu, Interfacial engineering of Co

nanoparticles/Co_2C nanowires boosts overall water splitting kinetics, Appl. Catal. B: Environ. 296 (2021) 120334.

[4] S.M. Li, L. Bai, H.B. Shi, X.F. Hao, L. Chen, X.J. Qin, G.J. Shao, Mo-doped CoP nanosheets as high-performance electrocatalyst for HER and OER, Ionics 27 (2021), 3109-3118.

[5] B.T. Jebaslinhepzybai, T. Partheeban, D.S. Gavali, R. Thapa, M. Sasidharan, One-pot solvothermal synthesis of Co_2P nanoparticles: an efficient HER and OER electrocatalysts, Int. J. Hydrogen Energy 46 (2021) 21924-21938.

[6] C.L. Huang, X.F. Chuah, C.T. Hsieh, S.Y. Lu, NiFe alloy nanotube arrays as highly efficient bifunctional electrocatalysts for overall water splitting at high current densities, ACS Appl. Mater. Interfaces 11 (2019) 24096-24106.

[7] A. Hanan, M.N. Lakhan, D. Shu, A. Hussain, M. Ahmed, I.A. Soomro, V. Kumar, D.X. Cao, An efficient and durable bifunctional electrocatalyst based on PdO and Co_2FeO_4 for HER and OER, Int. J. Hydrogen Energy 48 (2023) 19494-19508.

[8] K.B. Patel, B. Parmar, K. Ravi, R. Patidar, J.C. Chaudhari, D.N. Srivastava, G.R. Bhadu, Metal-organic framework derived core-shell nanoparticles as high performance bifunctional electrocatalysts for HER and OER, Appl. Surf. Sci. 616 (2023) 156499.

[9] D.E. Lee, S. Moru, K.P. Reddy, W.K. Jo, S. Tonda, Bimetallic Cu-Ni core-shell nanoparticles anchored N-doped reduced graphene oxide as a high-performance bifunctional electrocatalyst for alkaline water splitting, Appl. Surf. Sci. 622 (2023) 156928.

[10] X.Y. Wang, X. Yu, J.L. Bai, G.J. Yuan, P.Y. He, Y.Q. Zhu, S.Wu, F. Qin, L.L. Ren, Interface engineering assisted Fe-Ni_3S_2/Ni_2P heterostructure as a high-performance bifunctional electrocatalyst for OER and HER, Electrochim. Acta 458 (2023) 142524.

[11] S.F. Tan, W.M. yang, Y.J. Ji, Q.W. Hong, Carbon wrapped bimetallic NiCo nanospheres toward excellent HER and OER performance, J. Alloys Compd. 889 (2021) 161528.

[12] B. Chen, P. Hu, F. Yang, X.J. Hua, F.F. Yang, F. Zhu, R.Y. Sun, K. Hao, K. Wang, Z.Y. Yin, In situ porousized MoS_2 nano islands enhance HER/OER bifunctional electrocatalysis, Small 19 (2023) 2207177.

[13] H.L. Lin, N. Liu, Z.P. Shi, Y.L. Guo, Y. Tang, Q.S. Gao, Cobalt-doping in molybdenum-carbide nanowires toward efficient electrocatalytic hydrogen evolution, Adv. Funct. Mater. 26 (2016) 5590-5598.

[14] J.X. Diao, Y. Qiu, S.Q. Liu, W.T. Wang, K. Chen, H.L. Li, W.Y. Yuan, Y.T. Qu, X.H. Guo, Interfacial engineering of W_2N/WC heterostructures derived from solid-state synthesis: a highly efficient trifunctional electrocatalyst for ORR, OER, and HER, Adv. Mater. 32 (2020) 1905679.

[15] E. Vijayakumar, S. Ramakrishnan, C. Sathiskumar, D.J. Yoo, J. Balamurugan, H.S. Noh, D. Kwon, Y.H. Kim, H. Lee, MOF-derived CoP-nitrogen-doped carbon@NiFeP nanoflakes as an efficient and durable electrocatalyst with multiple catalytically active sites for OER, HER, ORR and rechargeable zinc-air batteries, Chem. Eng. J. 428 (2022) 131115.

[16] S.J. Sun, C.Y. Zhang, M.X. Ran, Y.J. Zheng, C.H. Li, Y. Jiang, X.M. Yan, Fe-doped promotes phosphorization and dispersibility of Ni catalysts for efficient and stable HER and OER, Int. J. Hydrogen Energy 63 (2024) 133-141.

All the DFT calculations were conducted based on the Vienna Ab-inito Simulation Package (VASP) [1-2]. The exchange-correlation effects were described by the Perdew-Burke-Ernzerhof (PBE) functional within the generalized gradient approximation (GGA) method [3-4]. The core-valence interactions were accounted by the projected augmented wave (PAW) method [5]. The energy cutoff for plane wave expansions was set to 500 eV, and the 3×3×1 Monkhorst-Pack grid k-points were selected to sample the Brillouin zone integration. The vacuum space is adopted 15 Å above the surfaces to avoid periodic interactions. The structural optimization was completed for energy and force convergence set at 1.0×10^{-4} eV and 0.02 eV $Å^{-1}$, respectively.

The Gibbs free energy change (ΔG) of each step is calculated using the following formula:

$$\Delta G = \Delta E + \Delta ZPE - T\Delta S$$

where ΔE is the electronic energy difference directly obtained from DFT calculations, ΔZPE is the zero point energy difference, T is the room temperature (298.15 K) and ΔS is the entropy change. ZPE could be obtained after frequency calculation by [6]:

$$ZPE = \frac{1}{2}\sum hvi$$

And the TS values of adsorbed species are calculated according to the vibrational frequencies [7]:

$$TS = k_B T \left[\sum_k ln(\frac{1}{1 - e^{-hv/k_B T}}) + \sum_k \frac{hv}{k_B T} \frac{1}{(e^{hv/k_B T} - 1)} + 1 \right]$$

References

[1] G. Kresse, J. Hafner, Ab initiomolecular dynamics for liquid metals, *Phys. Rev. B* 47 (1993) 558-561.

[2] G. Kresse, J. Hafner, Ab initiomolecular-dynamics simulation of the liquid-metal-amorphous-semiconductor transition in germanium, *Phys. Rev. B* 49 (1994) 14251-14269.

[3] J. P. Perdew, K. Burke, M. Ernzerhof, Generalized gradient approximation made simple, *Phys. Rev. Lett.* 77 (1996) 3865-3868.

[4] G. Kresse, D. Joubert, From ultrasoft pseudopotentials to the projector augmented-wave method, *Phys. Rev. B* 59 (1999) 1758-1775.

[5] P. E. Blöchl, Projector augmented-wave method, *Phys. Rev. B* 50 (1994) 17953-17979.

[6] Nørskov JK, Rossmeisl J, Logadottir A, Lindqvist L, Kitchin JR, Bligaard T, Jonsson H, Origin of the overpotential for oxygen reduction at a fuel-cell cathode, *J. Phys. Chem. B* 108 (2004) 17886–17892.

[7] Bendavid LI, Carter EA, CO_2 adsorption on Cu_2O(111): A DFT+U and DFT-D study, *J. Phys. Chem. C* 117 (2013) 26048–26059.